Phase and coherence extraction from a phased vertical cavity laser array

Matthew T. Johnson,[a] Dominic F. Siriani,[b] Joshua D. Sulkin,[c] and Kent D. Choquette
Micro and Nano Technology Laboratory, Department of Electrical and Computer Engineering, University of Illinois at Urbana-Champaign, Urbana, Illinois 61820, USA

(Received 2 April 2012; accepted 25 June 2012; published online 19 July 2012)

The relative coherence and phase are extracted from two-element, coherently coupled, vertical cavity surface emitting laser arrays. The array elements are defined optically by a photonic crystal pattern and electrically by ion implantation. We obtain the near and far fields experimentally under varying current injection. The Fraunhofer approximation is used to simulate propagation from the near to far field. The phase and coherence are extracted as fitting parameters to match the experimental and propagated far field patterns. The phase and coherence will aid in future array designs and in elucidating the phase-shifting mechanism. © *2012 American Institute of Physics*. [http://dx.doi.org/10.1063/1.4736406]

Two potential applications of phased vertical cavity surface emitting laser (VCSEL) arrays include beam-steering[1,2] and high-brightness sources. Non-mechanical optical beam steering promises lower cost, higher reliability, lower complexity, and higher speed than mechanical approaches, which are typically still the norm for applications such as laser radar. While prior methods of non-mechanical optical beam steering have been passive,[3] a phased VCSEL array uniquely acts as both the source and the phase-shifting mechanism. In this way, it represents a closer analog to its phased array radar counterpart, affording the potential for increased efficiency with decreased power consumption and complexity. While various methods of beam steering with VCSELs have been demonstrated, typical difficulties include wide beam width,[4] out-of-phase operation,[5,6] complex mechanical parts,[7] and discontinuous steering.[1] Recently, we have demonstrated continuous electronic beam steering with full, predictable coverage up to a 1° full angle with 19%–23% efficiency in the central lobe.[2]

Phased VCSEL arrays also offer a good alternative to edge emitting lasers as high brightness sources for applications such as fiber laser pumps. The major difficulty encountered with this approach[8,9] is that the typical evanescent coupling designs lead to nearest neighbor elements in the out-of-phase supermode, as was predicted,[10] leading to an undesirable 4-lobed far field pattern. While phase-corrected[11] and anti-guided (leaky mode)[12–17] VCSEL arrays have been shown to reliably produce in-phase coupling between elements, they require complicated etching and material re-growth processes. We have recently demonstrated coherent VCSEL arrays with reliable, anti-guided, in-phase coupling with much less fabrication complexity.[16–18] These arrays are designed to have photonic crystal optical confinement,[19] implant-defined current confinement,[17,18] and proper element spacing to preferentially select the in-phase mode.[17] If a large number of elements can be kept in-phase, VCSEL arrays have the potential to surpass edge-emitting lasers for high-brightness applications.

Common to both of these applications is the need to carefully control the phase difference between neighboring elements. In this work, the relative phase and optical coherence between 2×1 arrays are extracted by first experimentally determining the near and far field profiles as a function of injection current. The Fraunhofer approximation is used to simulate propagation from the near to far field. The phase and coherence are then extracted as fitting parameters to match the experimental and propagated far field patterns. While similar methods have been used with Fraunhoffer diffraction theory,[20] antenna array theory,[21,22] and the fast Fourier transform,[23] they typically use top-hat or Gaussian approximations for the near field. The technique demonstrated herein is particularly suited for extracting the relative phase and is unique in using the experimentally determined near field, which is shown to yield a more accurate simulation of the far field, and therefore more accurate phase information. The extracted phase and coherence will aid in future designs of phased VCSEL arrays, and in elucidating the physical mechanism(s) controlling them.

The VCSEL arrays under study are arranged in a 2×1 configuration where the fabrication procedure has been described in previous work.[17,18] The wafer consists of 27 p-type top and 35 n-type bottom distributed Bragg reflector periods on an n-type GaAs substrate. The active region consists of three GaAs quantum wells emitting nominally at 850 nm. The photonic crystal pattern etched into the top mirror limits the number of lasing modes and provides stable index guiding. The defects in the hole pattern create the array elements and are aligned with implant apertures approximately the same size. The latter confines the current to the individual elements, as shown in the cross section of Figure 1. In an additional step, the top metal contact was etched with a focused ion beam to allow preferential current injection into either array element.

Two types of array operation are analyzed, one that prefers to operate out-of-phase, and another that prefers to operate in-phase, as shown in Figure 2. The out-of-phase array is distinguished by a null in between the elements in the near field, while a small central lobe is apparent for the in-phase

[a]Electronic mail: mtjohns2@illinois.edu.
[b]Present address: MIT Lincoln Laboratory, Lexington, Massachusetts 02420, USA.
[c]Present address: Space Exploration Technologies, Hawthorne, California 90250, USA.

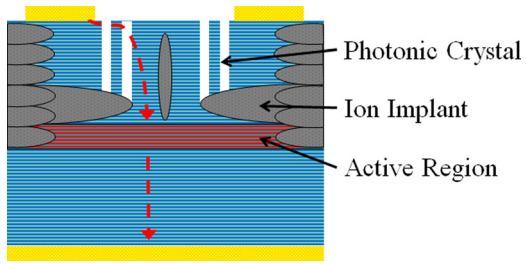

FIG. 1. Cross section of VCSEL array. Dashed line shows preferential current path from left contact.

array.[18] Near fields images are first acquired with a microscope under varying current injection. The verification process showed that a greater number of pixels on the near field image, up to the microscope objective resolution, yield a more accurate far field calculation. This process also revealed the need to adjust the camera exposure time to ensure the maximum dynamic range for each near field image, while avoiding saturation.

The near field images are then processed to truncate the noise and split them into different apertures, as shown in Figures 2(c) and 2(f). The three-aperture case for the in-phase array is detailed here. The electric field amplitudes for each aperture are obtained as the square root of the measure intensity, and are defined as $|U_{left}(\xi,\eta)|$, $|U_{mid}(\xi,\eta)|$, and $|U_{right}(\xi,\eta)|$, where ξ and η are the near-field coordinates. Approximating these fields as self-coherent and monochromatic with flat wavefronts, the beam was then "propagated" to the far field using the Fraunhofer approximation[24]

$$U(x,y) = \frac{e^{jk_0 z}}{j\lambda z} e^{j\frac{k_0}{2z}(x^2+y^2)} \int\int_{-\infty}^{\infty} |U(\xi,\eta)| e^{j\frac{2\pi}{\lambda z}(x\xi+y\eta)} d\xi d\eta, \quad (1)$$

where x and y are the far field coordinates, z is the propagation distance, and k_0 and λ correspond to the free space wavelength. This approximation conveniently lends itself to a two-dimensional Fourier transform, which can be quickly solved. For a three-element array, the relative phase of the right aperture, Φ_{right}, and its relative coherence, γ, can then be fit according to

$$I(x,y) = |U_{left}(x,y)|^2 + |U_{mid}(x,y)|^2 + |U_{right}(x,y)|^2 + 2|\gamma|\mathrm{Re}\begin{bmatrix} U_{left}(x,y)^* U_{right}(x,y) e^{j\Phi_{right}} \\ +U_{left}(x,y)^* U_{mid}(x,y) e^{j\Phi_{mid}} \\ +U_{mid}(x,y) e^{-j\Phi_{mid}} U_{right}(x,y) e^{j\Phi_{right}} \end{bmatrix}, \quad (2)$$

where the propagated far field intensity is denoted as $I(x,y)$, the relative phase of the middle aperture as Φ_{mid}, and the far fields propagated from the left, middle, and right apertures as $U_{left}(x,y)$, $U_{mid}(x,y)$, and $U_{right}(x,y)$, respectively. Since there is a typical π phase difference between adjacent near field lobes in phased VCSEL arrays,[12] Φ_{mid} is assumed to be π out of phase with the average phase of the two outer apertures. The parameters Φ_{right} and γ can then be extracted by matching the experimentally determined far field with that propagated from the near field, according to Eqs. (1) and (2). The relative phase is first determined in an iterative process until the relative amplitudes of the left and right far field lobes match those determined experimentally. This method was used in contrast to that of previous works[21,22] where the angular shifts are matched, as the latter is not only subject to greater experimental error, but can be affected by minute frequency splitting between the elements as well.[25] Similarly, the coherence was determined by matching the relative amplitude of the center nulls. The coherence is thus obtained from both the visibility in the far field as well as the relative intensities of the near field elements.

Near and far-field measurements are taken over the range of coherent operation of each array for fixed current injection through the left, and varying current injection into the right contact. The propagated-fit and experimental far field profiles are compared for the out-of-phase and in-phase arrays in Figures 3(a) and 3(b), respectively, where the 2D insets show the slices where the 1D profiles are taken. Good agreement is shown between the experimental and propagated-fit far field patterns. Figure 3(b) also shows the profile that was obtained by using a best-fit Gaussian

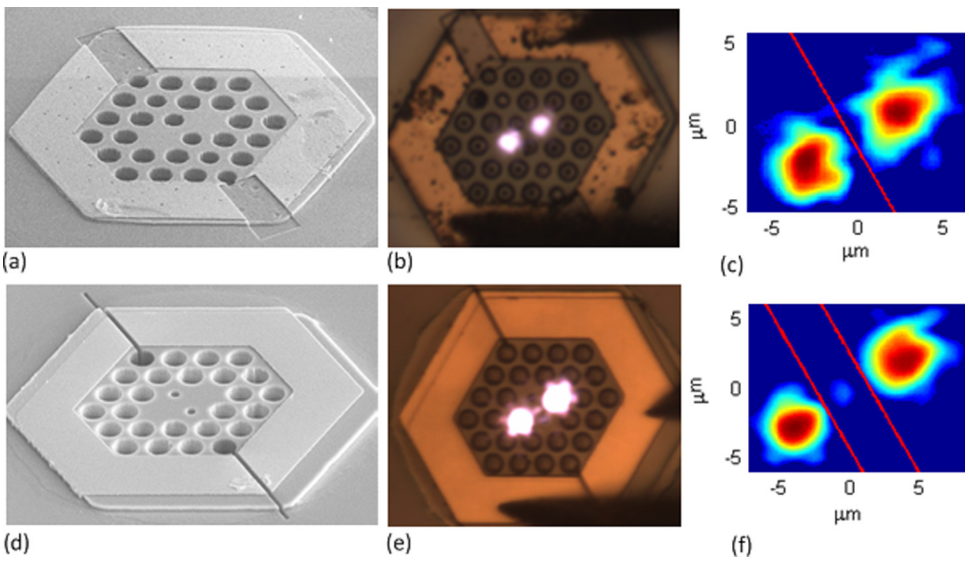

FIG. 2. Out-of-phase (a-c) and in-phase (d-f) VCSEL arrays. Images from an SEM (a,d), while lasing (b,e), and of the processed near field (c,f), where the red lines delineate the apertures used for simulation.

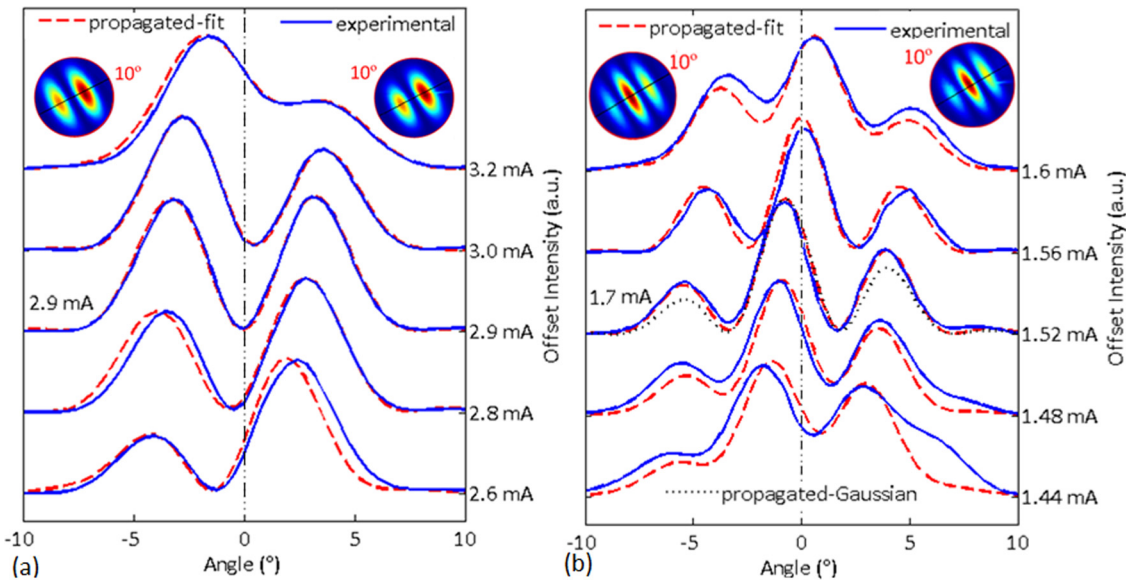

FIG. 3. Far field profiles for arrays operating out-of-phase (a) and in-phase (b) under current injection to the left and right apertures shown on the left and right of each plot, respectively. The propagated-Gaussian profile in (b) shows the decrease in accuracy when a best-fit Gaussian approximation is used for the array elements in the near field. Profiles taken along slices are shown in 2D insets.

approximation for $U_{left}(\xi,\eta)$ and $U_{right}(\xi,\eta)$, while ignoring the small central lobe shown in Figure 2(f). While the far field profile of the "propagated-Gaussian" looks similar to that obtained experimentally, its outer lobe intensities are noticeably smaller. This difference is magnified for in-phase VCSEL arrays with larger near-field central lobes,[18] and is due to the significant impact this out-of-phase central lobe has on the far field. Including this central lobe thus leads to a more accurate far field simulation, and therefore more accurate phase information retrieved by matching the intensities of the outer far-field lobes.

In both arrays, it can be seen that as the current to the right aperture is increased, the far field is pulled to the right. This is caused by a linearly increasing relative phase lag in the right element, as plotted in Figures 4(a) and 4(b). Note that the observed phase range of coherent operation for both arrays extends about 0.5π in either direction of their preferred phase relation. Beyond this phase range, the in-phase (out-of-phase) array approaches out-of-phase (in-phase) operation, which leads to a dramatic decrease in coherence.[26]

Both of the arrays display several orders of magnitude greater sensitivity to current than shown for phase-tuning in slab-coupled lasers.[27] The out-of-phase array operates over a differential current spread of 0.6 mA, while the in-phase array operates over a smaller range of 0.17 mA. This difference is due to a deeper etch between the contacts for the in-phase array, as is slightly noticeable in the SEM images of Figure 2. The resistance between the left and right contacts for the in-phase array was 6.3 kΩ, compared to 2.6 kΩ for the out-of-phase array, yielding much better current confinement between the array elements. This current confinement was also observable in the spectrum. The lasing wavelengths of the two elements were matched when similar current was applied to each, but their wavelengths split wider and wider with increased current difference. This is caused by localized current and temperature differences between the elements, which cause an index variation in the active region (cavity).

The coherence magnitude and wavelength are also plotted against the current difference in Figures 4(a) and 4(b). While both arrays are highly coherent around their preferred mode of operation (0 or π phase difference), they lose coherence as they are pulled away from it. This loss of coherence is also associated with the onset of a competing mode, as shown by the spectra. This corroborates previous results

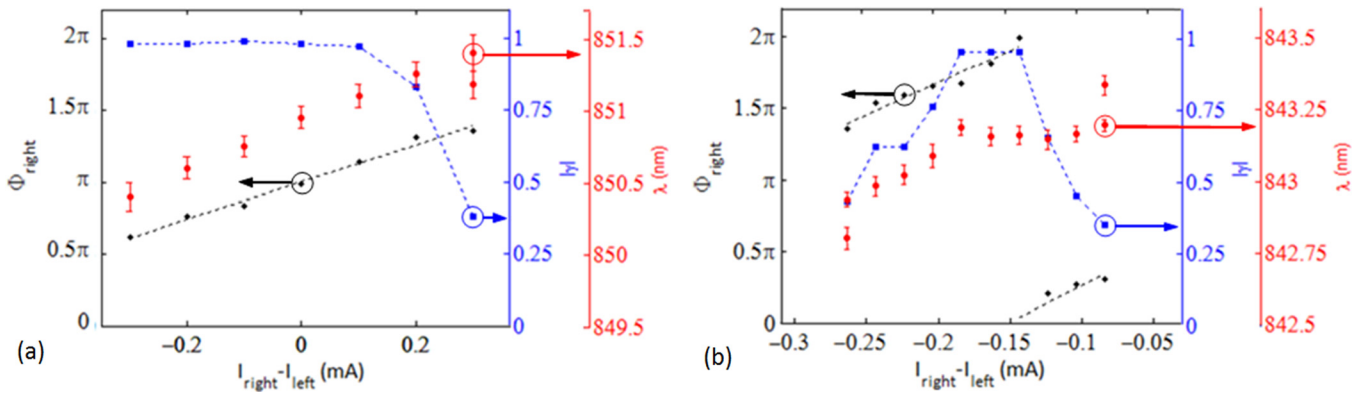

FIG. 4. Phase, coherence, and wavelength vs. current injection difference for the (a) out-of-phase and (b) in-phase VCSEL array.

showing a reduction in coherence when operated away from the preferred in-phase or out-of-phase condition,[26] and upon the onset of another spectral mode.[28]

In conclusion, the Fraunhofer approximation is applied to extract the relative phase and coherence of a two-element VCSEL array. The experimentally determined near-field is used (as opposed to a top-hat or Gaussian approximation) and the far field lobe intensities are matched (as opposed to the angular shifts), to obtain maximum accuracy. The relative phase difference of the VCSEL array elements is found to vary over a range of π for both arrays. As current injection into a given element is increased, its relative phase is found to increasingly lag. Additionally, the array coherence is found to dramatically decrease as an array's preferred phase relationship is pulled beyond 0.5π in either direction.

A two-pinhole optical setup or implementation of a Gerchberg-Saxton algorithm would provide a more rigorous coherence and phase mapping across the array without relying on the assumption that each aperture was self-coherent with a flat wavefront. The good agreement between the experimental and propagated-fit far-fields for the arrays studied, however, offers confirmation of our more convenient method and its underlying assumptions. Future work will include dynamic characterization of the phased VCSEL arrays and investigation into the phase-shifting mechanism(s).

This work was partially supported by the Navy SBIR N11A-024-0476.

[1]A. C. Lehman, D. F. Siriani, and K. D. Choquette, Electron. Lett. **43**(22), 1202 (2007).
[2]D. F. Siriani and K. D. Choquette, IEEE Photon. Technol. Lett. **23**, 167–169 (2011).
[3]P. F. McManamon, P. J. Bos, M. J. Escuti, J. Heikenfeld, S. Serati, H. Xie, and E. A. Watson, Proc. IEEE **97**, 1078 (2009).
[4]T. Ide, M. Shimizu, S. Mukai, M. Ogura, T. Kikuchi, Y. Suzuki, R. Kaji, H. Itoh, M. Watanabe, and H. Yajima, Jpn. J. Appl. Phys Part 1 **38**, 1966 (1999).
[5]M. I. Cohen, A. A. Allerman, K. D. Choquette, and C. Jagadish, IEEE Photon. Technol. Lett. **13**, 544 (2001).
[6]L. D. A. Lundeberg and E. Kapon, Appl. Phys. Lett. **90**, 241115 (2007).
[7]A. Tuantranont, V. M. Bright, J. Zhang, W. Zhang, J. A. Neff, and Y. C. Lee, Sens. Actuators, A **91**, 363 (2001).
[8]M. Orenstein, E. Kapon, J. P. Harbison, L. T. Florez, and N. G. Stoffel, Appl. Phys. Lett. **60**, 1535 (1992).
[9]R. A. Morgan, K. Kojima, T. Mullally, G. D. Guth, M. W. Focht, R. E. Leibenguth, and M. Asom, Appl. Phys. Lett. **61**, 1160 (1992).
[10]G. R. Hadley, Opt. Lett. **15**, 1215 (1990).
[11]M. E. Warren, P. L. Gourley, G. R. Hadley, G. A. Vawter, T. M. Brennan, B. E. Hammons, and K. L. Lear, Appl. Phys. Lett. **61**, 1484 (1992).
[12]D. K. Serkland, K. D. Choquette, G. R. Hadley, K. M. Geib, and A. A. Allerman, Appl. Phys. Lett. **75**, 3754 (1999).
[13]D. Zhou and L. J. Mawst, Appl. Phys. Lett. **77**, 2307 (2000).
[14]D. Zhou, L. J. Mawst, and Z. Dai, IEEE J. Quantum Electron. **38**, 652 (2002).
[15]L. Bao, N. H. Kim, L. J. Mawst, N. N. Elkin, V. N. Troshchieva, D. V. Vysotsky, and A. P. Napartovich, Appl. Phys. Lett. **84**, 320 (2004).
[16]D. F. Siriani and K. D. Choquette, Electron. Lett. **46**, 712 (2010).
[17]D. F. Siriani and K. D. Choquette, IEEE J. Quantum Electron. **47**, 160 (2011).
[18]A. C. Lehman and K. D. Choquette, IEEE Photon. Technol. Lett. **19**, 1421 (2007).
[19]J. J. Raftery, Jr., A. C. Lehman, A. J. Danner, P. O. Leisher, A. V. Giannopoulos, and K. D. Choquette, Appl. Phys. Lett. **89**, 081119 (2006).
[20]P. K. Cheo, A. Liu, and G. G. King, IEEE Photon. Technol. Lett. **13**, 439 (2001).
[21]A. C. Lehman, J. J. Raftery, Jr., A. J. Danner, P. O. Leisher, and K. D. Choquette, Appl. Phys. Lett. **88**, 021102 (2006).
[22]L. D. A. Lundeberg, G. P. Lousberg, D. L. Boiko, and E. Kapon, Appl. Phys. Lett. **90**, 021103 (2007).
[23]J. W. Shi, J. L. Yen, C. H. Jiang, K. M. Chen, T. J. Hung, and Y. J. Yang, IEEE Photon. Technol. Lett. **18**, 481 (2006).
[24]J. W. Goodman, *Introduction to Fourier Optics* (Roberts & Company Publishers, 2005).
[25]A. C. Lehman Harren, K. D. Choquette, and P. S. Carney, Opt. Lett. **34**, 905 (2009).
[26]A. C. Lehman, J. J. Raftery, P. S. Carney, and K. D. Choquette, IEEE J. Quantum Electron. **43**, 25 (2007).
[27]R. K. Huang, B. Chann, L. J. Missaggia, S. J. Augst, M. K. Connors, G. W. Turner, A. Sanchez-Rubio, J. P. Donnelly, J. L. Hostetler, and C. Miester, Proc. SPIE **7230**, 72301G (2009).
[28]D. F. Siriani, P. S. Carney, and K. D. Choquette, IEEE J. Quantum Electron. **47**, 672 (2011).